

Diffusion of gold nanoclusters on graphite

Laurent J. Lewis,^(a)

Département de Physique et Groupe de Recherche en Physique et Technologie des Couches Minces (GCM), Université de Montréal, Case Postale 6128, Succursale Centre-Ville, Montréal, Québec, Canada H3C 3J7

Pablo Jensen,^(b) Nicolas Combe,^(c) and Jean-Louis Barrat^(d)

Département de Physique des Matériaux, Université Claude-Bernard Lyon-I, CNRS UMR 5586, 69622 Villeurbanne Cédex, France

(August 10, 2018)

Submitted to *Physical Review B*

We present a detailed molecular-dynamics study of the diffusion and coalescence of large (249-atom) gold clusters on graphite surfaces. The diffusivity of monoclusters is found to be comparable to that for single adatoms. Likewise, and even more important, cluster dimers are also found to diffuse at a rate which is comparable to that for adatoms and monoclusters. As a consequence, large islands formed by cluster aggregation are also expected to be mobile. Using kinetic Monte Carlo simulations, and assuming a proper scaling law for the dependence on size of the diffusivity of large clusters, we find that islands consisting of as many as 100 monoclusters should exhibit significant mobility. This result has profound implications for the morphology of cluster-assembled materials.

PACS numbers: 36.40.Sx, 61.46.+w, 68.35.Fx, 07.05.Tp

I. INTRODUCTION

Nanometer-size clusters — or simply nanoclusters — are intrinsically different from bulk materials.^{1,2} Yet, understanding of several of their most fundamental physical properties is just beginning to emerge (see for instance Refs. 3–9), thanks largely to rapid progresses in the technology of fabrication and analysis, but also considerable advances in computational tools and methodology.

It has recently been demonstrated^{10–12} that depositing clusters (rather than single atoms) on surfaces allow the fabrication of interesting nanostructured materials whose properties can be tailored to specific technological applications, e.g., micro-electronic, optoelectronic, and magnetic devices.¹³ If single-atom deposition is used, the nanostructures have to be grown directly on the substrate through diffusion and aggregation, which depends in a detailed (and in general very complicated) manner on the interactions between surface atoms and adatoms. By contrast, for cluster deposition, the clusters are prepared before they hit the surface, giving considerably more flexibility¹⁴ in assembling or organizing clusters for particular applications. It has been shown, for instance, that by changing the mean size of the incident carbon clusters, it was possible to modify the structure of the resulting carbon film from graphitic to diamond-like.¹⁰ This however requires that sufficient control over the cluster deposition and subsequent growth process be achieved.^{11,12}

Diffusion evidently plays a central role in the fabrication of thin films and self-organized structures by clus-

ter deposition. It has been demonstrated experimentally that gold or antimony clusters diffuse on graphite surfaces at a surprisingly high rate of about 10^{-8} cm²/s at room temperature,¹⁵ quite comparable to the rates that can be achieved by single atoms in similar conditions. This was confirmed theoretically by Deltour *et al.* using molecular-dynamics simulations:⁷ clusters consisting of particles which are incommensurate with the substrate exhibit very rapid diffusion. The cluster diffuses “as a whole”, and its path is akin to a Brownian motion induced by the internal vibrations of the clusters and/or the vibrations of the substrate. This is in striking contrast with other cluster diffusion mechanisms, whereby the motion results from a combination of single-atom processes, such as evaporation-condensation, edge diffusion, etc. The latter mechanisms are more appropriate to clusters which are in epitaxy with the surface, and are likely not significant in cases where the mismatch is large and/or the substrate-cluster interactions are weak, such as in Refs. 15 and 16 (see Ref. 12 for a review).

In the present paper, we re-examine the problem of cluster diffusion in the cluster-substrate-mismatched case, now using a much more accurate model: indeed, in the work of Deltour *et al.*,⁷ cluster-cluster, cluster-substrate and substrate-substrate interactions were all assumed to be of the Lennard-Jones form, which cannot be expected to correctly describe “real materials”. Here, we consider a simple, but realistic model for the diffusion of gold clusters on a graphite surface (HOPG). We are concerned with gold because it has been the object of several experimental studies,^{12,17–19} but also be-

cause realistic semi-empirical, many-body potentials are available for this material. The energetics of gold atoms is described in terms of the embedded-atom-method (EAM),²⁰ while carbon atoms are assumed to interact via Tersoff potentials;²¹ the (weak) interactions between gold and carbon atoms are modeled with a simple Lennard-Jones potential. A comparable model was used recently by Luedtke and Landman to study the anomalous diffusion of a gold nanocluster on graphite;⁹ diffusion was found to proceed via a stick-slip mechanism, resulting in an apparent Lévy-flight type of motion. In the present work, we examine closely the variations with temperature of the rate of diffusion, as well as the microscopies of cluster dimers (diclusters).

We find the diffusivity of monoclusters to be entirely comparable to that for single adatoms. Likewise, and most important, diclusters are also found to diffuse at a rate which is comparable to that for adatoms and monoclusters. It is therefore expected that large islands, formed by the aggregation of many clusters, should also be mobile. Based on this observation, we carried out kinetic Monte Carlo simulations of island diffusion and coalescence assuming a proper scaling law for the dependence on size of the diffusivity of large clusters. We find that islands consisting of as many as 100 monoclusters exhibit significant mobility; this is consistent with the observation on graphite of large (200 monoclusters) gold islands. The morphology of cluster-assembled materials is profoundly affected by the mobility of multi-cluster islands.

II. COMPUTATIONAL DETAILS

Diffusion coefficients for clusters can only be obtained at the expense of very long MD runs: there exists numerous possible diffusion paths, and there is therefore not a single energy barrier (and prefactor) characterizing the dynamics. These systems, further, do not lend themselves readily to accelerated MD algorithms.^{22,23} Brute-force simulations – long enough for statistically-significant data to be collected – therefore appear to be the only avenue. This rules out *ab initio* methods, which can only deal with very small systems (a few tens of atoms) over limited timescales (tens of picoseconds at best): empirical or semi-empirical potentials *must* be employed.

As mentioned above, we describe here the interactions between Au particles using the embedded-atom method (EAM),²⁰ an *n*-body potential with proven ability to describe reliably various static and dynamic properties of transition and noble metals in either bulk or surface configurations.²⁴ The model is “semi-empirical” in the sense that it approaches the total-energy problem from a local electron-density viewpoint, but using a functional form with parameters fitted to experiment (equilibrium lattice constant, sublimation energy, bulk modulus, elas-

tic constants, etc.).

The interactions between C atoms are modelled using the Tersoff potential,²¹ an empirical *n*-body potential which accounts well for various conformations of carbon. The Tersoff potential for carbon is truncated at 2.10 Å, which turns out to be smaller than the inter-plane distance in graphite, 3.35 Å. Thus, within this model, there are no interactions between neighbouring graphite planes. This is of course an approximation, but not a bad one since basal planes in graphite are known to interact weakly. (This is why it is a good lubricant!). A pleasant consequence of this is that the substrate can be assumed to consist of a single and only layer, thus reducing formidably the (nevertheless very heavy) computational load of the calculations.

Last — and most problematic — is the Au-C interaction, for which no simple (empirical or semi-empirical) model is to our knowledge available. One way of determining this would be to fit an *ab initio* database to a proper, manageable functional potential. However, since Au-C pairs conform in so many different ways in the present problem, this appears to be a hopeless task, not worth the effort in view of the other approximations we have to live with. We therefore improvised this interaction a little bit and took it to be of the Lennard-Jones form, with $\sigma = 2.74$ Å and $\epsilon = 0.022$ eV, truncated at 4.50 Å. The parameters were determined rather loosely from various two-body models for Ag-C and Pt-C interactions.²⁵ Overall, we expect our model to provide a *qualitatively correct* description of the system, *realistic* in that the most important physical characteristics are well taken into account. It is however not expected to provide a quantitatively *precise* account of the particular system under consideration, but should be relevant to several types of metallic clusters which bind weakly to graphite.

We consider here gold nanoclusters comprising 249 atoms, a size which is close to that of clusters deposited in the experiments.^{12,19} The graphite layer has dimensions 66.15×63.65 Å² and contains 1500 atoms. Calculations were carried out for several temperatures in the range 400–900 K. It should be noted that a free-standing 249-atom Au cluster melts at about 650 K in this model.⁶ This temperature is not affected in a significant manner by the graphite substrate as the interaction between Au and graphite-C atoms are weak. However, the dynamics of the cluster is expected to be different in the high-temperature molten state and the low-temperature solid state. All simulations were microcanonical, except for the initial thermalisation period at each temperature; no drift in the temperature was observed.

Simulations were carried out in most cases using a fully dynamical substrate. In two cases, one for the single cluster and the other for the dicluster, extremely long runs using a static (frozen) substrate were performed: it has been found by Deltour *et al.*⁷ that diffusion is quantitatively similar on both substrates (however, see Section III B below). The equations of motion were in-

tegrated using the velocity form of the Verlet algorithm with a timestep of 1.0 and 2.5 fs for dynamic and static substrates, respectively.²⁶ (Carbon being a light atom, a smaller timestep is needed in order to properly describe the motion). The dynamic-substrate simulations ran between 10 and 14 million timesteps (depending on temperature), i.e., 10–14 ns. The static-substrate simulation for the monocluster, in comparison, ran for a total of 50 million timesteps, i.e., a very respectable 125 ns = 0.125 μ s; the corresponding dicluster simulation ran for 75 ns. All calculations were performed using the program **groF**, a general-purpose MD code for bulk and surfaces developed by one of the authors (LJL).

III. RESULTS

A. Dynamic-substrate simulations

We first discuss diffusion on a dynamic substrate, i.e., with *all* parts of the system explicitly dealt with in the MD simulations. Fig. 1 gives the (time-averaged) mean-square displacements (MSD's) of the cluster's center-of-mass at the various temperatures investigated, which will be used to calculate the diffusion constant, $D = \lim_{t \rightarrow \infty} r^2(t)/4t$. As indicated above, the simulations extend over 10–14 ns, but the MSD's are only shown for a maximum correlation time of one ns in order to “ensure” statistical reliability. It is evident (e.g., upon comparing the results at 700 and 800 K) that the diffusion coefficients that can be extracted from these plots will carry a sizeable error bar. Nevertheless, it is certainly the case that (i) diffusion is *very significant* and (ii) it increases rapidly with temperature.

There is no evidence from these plots that the MSD's obey a non-linear power law behaviour (i.e., that the cluster undergoes superdiffusion) which could be associated with “Lévy flights”: the statistical accuracy of the data is simply not sufficient to draw any conclusions. The cluster does however undergo long jumps during the course of its motion. We will return to this point below when we discuss diffusion on a frozen substrate.

In lack of a better description of the long-time behaviour of the diffusion process, we simply assume that $r^2(t) \rightarrow 4Dt$ as t gets large. The resulting diffusion coefficients are plotted in the manner of Arrhenius, i.e., $\log D$ vs $1/k_B T$, in the inset of Fig. 1. If the process were truly Arrhenius, all points would fall on a single straight line. This is evidently not the case here. Though we could probably go ahead and fit the data to a straight line, attributing the discrepancies to statistical error, there is probably a natural explanation for the “break” that a sharp eye can observe between 600 and 700 K: As noted above, the free Au₂₄₉ cluster melts at about 650 K in the EAM model.⁶ The presence of the substrate raises the melting point, but very little since the interactions between the cluster and the graphite surface are small.

Thus, the cluster is solid at the lowest temperatures (400, 500 and 600 K), but liquid above (700, 800 and 900 K). The statistics are evidently insufficient to allow firm conclusions to be drawn; there nevertheless appears to be a discontinuity near the cluster melting point temperature, with activation energies on either side of about 0.05 eV. We discuss in Section III D the implications of these findings on the kinetics of growth.

B. Static-substrate simulations

The static-substrate simulations, carried out at a single temperature (for the cluster), *viz.* 500 K, serve many purposes: (i) re-assess the equivalence with dynamic-substrate MD runs reported by Deltour *et al.*;⁷ (ii) provide accurate statistics for a proper comparison of the diffusive behaviour of mono- and diclusters; (iii) examine the possible superdiffusive character of the trajectories.

We focus, first, on a comparison between static- and dynamic-substrate simulations. As can be appreciated from the MSD's given in the inset of Fig. 2, there is a rather substantial difference between the two calculations: for the dynamic substrate at 500 K, the diffusion constant is 3.71×10^{-5} cm²/s, while for the frozen substrate we have 1.09×10^{-5} cm²/s. (This value is actually significantly smaller than that for the dynamic substrate at 400 K — 100 K lower temperature — *viz.* 1.70×10^{-5} cm²/s). Again, statistical uncertainties cannot be totally excluded to account for this discrepancy, but it is difficult to imagine that it could explain all of the observed difference (cf. inset to Fig. 1 for a better appreciation of this difference). The explanation might however be quite simple.

As noted above, the cluster-substrate interactions are weak, and this likely plays an important role in determining the characteristics of the motion. Visual inspection of the $x - y$ paths in the two different situations makes it apparent that the motion has a much stronger “stick-and-jump” character on the frozen substrate than on the dynamic one. On the frozen substrate, further, the trajectory is more compact on a given timescale. This can in fact be characterized in a quantitative manner by considering, following Luedtke and Landman,⁹ the function $P_\tau(d)$, which gives the distribution of displacements of length d over a timescale of τ . The motion is best characterized using a value of τ corresponding to the period of vibration of the cluster in a sticking mode (see below).

The function $P_\tau(d)$ (normalized to unity) is displayed in Fig. 3 for the dynamic substrate at three different temperatures (400, 500, and 900 K) and for the static substrate at 500 K. The value of τ was determined from the frozen-substrate simulations by simply counting the number of oscillations over a given period of time; we found $\tau = 20$ ps to within about 10%. We note that, for the dynamic substrate, the period of oscillations at 400 K is about 38 ps, while no oscillations can be found at

500 and higher temperatures, i.e., the sticking mode is absent above 500 K or so.

The difference between static and dynamic substrates is striking: On the dynamic surface, $P_r(d)$ is a broad featureless distribution, which gets broader as temperature increases. The maximum of the distribution at low temperature lies at about 1.6–1.8 Å — roughly the distance between equilibrium sites on the graphite surface — clearly establishing that the motion proceeds in an quasi continuous manner via “sliding hops” to nearest-neighbours; the hops get longer as temperature increases. On the static substrate, in contrast, a “sticky” vibrational mode, of amplitude roughly 0.25 Å, is clearly visible. This is followed by a broad tail which corresponds, again, to the sliding jumps that are characteristic of the motion on the dynamic substrate.

Sticking, therefore, is much more likely to take place on the static than on the dynamic substrate, thereby contributing to decrease the average distance traveled by the cluster over a given period of time. This conclusion is however not general: The system under consideration here is perhaps a bit peculiar in that the cluster-substrate interactions are especially weak. (In comparison, Luedtke and Landman’s ϵ for the Au-C interaction is 0.01273 eV, even smaller than our own value.) One may conjecture that the vibrations of the surface are enough, in such cases, to overcome *completely* the barrier opposing diffusion, which might not be true of systems where the interactions are stronger (as in the case, e.g., of Deltour *et al.*’s simulations, Ref. 7).

It also appears that our diffusion data do not cover a timescale long enough to warrant firm conclusions to be drawn on the possibility that superdiffusion might be taking place. This is certainly true, as we have seen above, of the dynamic-substrate simulations, which cover “only” 10–14 nanoseconds, but also of the static-substrate simulations (assuming, in view of the above discussion, that they are relevant to the problem under study), which extend to 125 ns. Certainly, the position of the cluster’s center-of-mass does exhibit something of a self-similar character, as reported by Luedtke and Landman⁹, and as can be seen in Fig. 4. Evidently, one cannot trust statistics here over more than a decade or two in time. One might hope that superdiffusion would be more apparent in the long-time behaviour of the MSD’s. To this effect, we plot in Fig. 2 $\log r^2(t)$ vs $\log t$, for a maximum correlation time of (here) 40 ns;²⁷ the slope of such a plot is the diffusivity exponent γ . The statistical quality of the data decreases with correlation time, and becomes clearly insufficient over 5 ns or so; the large dip at about 15 ns can testify. Our best estimate of the slope γ at “large” (more than ~ 1 ns) correlation times is anywhere between 0.9 and 1.2, i.e., mild underdiffusion or mild superdiffusion... or no superdiffusion at all! This is consistent with the value reported by Luedtke and Landman, who find $\gamma = 1.1$ based on an analysis of sticking and sliding times. One point worth mentioning is that the velocity-autocorrelation function for adatom diffusion in the in-

termediate and high-friction regimes has been shown to follow a power-law behaviour at intermediate times; the exponential dependence resumes at very long times.²⁸

C. Diclusters

The morphology of films grown by cluster deposition depends critically on the coefficient of diffusion of monoclusters, as we have just seen, but also, because clusters aggregate, on the coefficient of diffusion of multicusters. From simple geometric arguments, it might be argued that the rate of diffusion should scale as $N^{-2/3}$, where N is the number of atoms in the cluster, as was in fact observed by Deltour *et al.*⁷ for Lennard-Jones clusters. However, it can be expected that the morphology of the films depends, as well, on the *shape* of the multi-clusters following the aggregation of monoclusters, i.e., on the kinetics of coalescence.

In a previous publication,⁶ we examined the coalescence of gold nanoclusters in vacuum and found it to be much slower than predicted by macroscopic theories. This state of affairs can be attributed to the presence of facets and edges which constitute barriers to the transport of particles required for coalescence to take place²⁹. The “neck” between two particles was however found to form very rapidly. We conjectured that these conclusions would apply equally well to the particular case of gold nanoclusters on graphite since the gold-graphite interactions are weak.

We have verified this in the context of the present work: indeed, coalescence is little affected by the presence of the substrate, as demonstrated in Fig. 5. We considered both a free-standing and a supported pair of 249-atom gold clusters. Starting at very low temperature (50 K), temperature was slowly and progressively (stepwise) raised to 600 K. (As noted above, the 249-atom gold cluster melts at about 650 K in this EAM model and we therefore did not go beyond this point). We plot, in Fig. 5, the evolution with time-temperature of the three moments of inertia of the dicluster. Since the cluster can rotate, the moments of inertia provide a more useful measure of the shape of the object than, e.g., the radii of gyration.⁶ A side view of the dicluster at 200 K, i.e., after the neck between the two monoclusters has formed completely, is shown in Fig. 6. It is evident that the dicluster does not wet the surface, and therefore the substrate plays a relatively minor role in the coalescence process.

As can be seen in Fig. 5, the behaviour of the free-standing and supported diclusters are almost identical, except for the initial phase of coalescence: the supported cluster forms a neck much more rapidly than the free-standing cluster, presumably because the substrate offers, through some thermostatic effect, an additional route via which coalescence (by plastic deformation) can be mediated; it is conceivable also that the substrate “forces” the atomic planes from the two clusters to align.

We have not explored these questions further; it remains that the end points of the two coalescence runs are identical within statistical uncertainty. Thus, again, coalescence is hampered by the presence of facets and edges; the timescale for complete coalescence is much longer than predicted by continuous theories. The shape of islands on the graphite surface will be strongly affected, and it is also expected that the rate of diffusion will be affected (since it is determined by the contact area between substrate and cluster).

The MSD of the dicluster (after proper equilibration at 500 K) is displayed in the inset of Fig. 2. As mentioned earlier, this was calculated from a static-substrate run covering 75 ns. The same limitations as noted above for the monocluster should therefore hold in the present case. It is a very remarkable (and perhaps even surprising) result that the rate of diffusion of the dicluster is quite comparable to that of the monocluster, inasmuch as the frozen-substrate simulations are concerned. (We expect the diffusion constants on the dynamic substrate to be different — and larger — but in a proportion that would be quite comparable to that found here). The value of $D = 1.38 \times 10^{-5} \text{ cm}^2/\text{s}$ we obtain for the dicluster is in fact a bit larger than that for the monocluster ($1.09 \times 10^{-5} \text{ cm}^2/\text{s}$). The difference is probably not meaningful; what *is* meaningful, however, is that the mono- and the dicluster have comparable coefficients of diffusion; this has profound implications on growth, as we discuss in Section III D, below.

The function $P(d)$ for the dicluster at 500 K is displayed in Fig. 3; here we estimate that $\tau = 40 \text{ ps}$ (vs about 20 ps for the monocluster). The distribution is quite similar to that found for the single cluster on the frozen substrate, though broader and shifted to slightly larger displacements. This last result is likely due to the fact that, being larger, the dicluster is not as easily able to accommodate itself with the substrate as the monocluster; in this sense, it is more loosely bound to the substrate.

D. Comparison with experimental results

Deposition of gold clusters on graphite experiments were carried out in Lyon recently.^{12,19} Several models have been proposed to extract the microscopic cluster diffusion coefficients from the measured island densities.¹² Of course, in order to provide a meaningful interpretation of the data, the models must take into account the precise conditions in which the experiments are performed. In Lyon, for instance, the flux of clusters is chopped, rather than continuous, and this affects the kinetics of diffusion and growth considerably.^{30,31} Previous estimates of the rates of diffusion of Au on graphite, which overlooked this important detail, are therefore in error. In Ref. 19, a diffusion coefficient of $10^{-3} \text{ cm}^2/\text{s}$ at 400 K is given; for a discussion, see Ref. 12. The “correct” number, in-

cluding flux chopping, would be $1.0 \text{ cm}^2/\text{s}$ if monoclusters only were assumed to be mobile. However, as we have seen above, cluster dimers diffuse at a rate which is quite comparable to that for monoclusters, suggesting that larger clusters would diffuse as well. The Lennard-Jones simulations of Deltour *et al.*⁷ indicate that the rate of diffusion of compact N -atom clusters scales roughly as the inverse of the contact area between the cluster and the substrate: $D_N = D_1 N^{-2/3}$. (Compact clusters are expected to form through aggregation and coalescence; see Ref. 12).

Experimentally, however, it is almost impossible to determine whether or not multiclusters do diffuse, and at which rate. In view of this, and the expected importance of multicluster mobility on growth, we have carried out a series of kinetic Monte Carlo (KMC) simulations in order to estimate the largest island which must be allowed to diffuse in order to account for the experimentally-observed gold island density on graphite at 400 K, viz. $4 \times 10^8 \text{ islands/cm}^2$, or 1.1×10^{-5} per site.^{12,19} To do so, we assume that the diffusion constant for monoclusters found in the present simulations is correct, and that the rate of diffusion of N -clusters scales according to the law given above. All other parameters (incident cluster flux, temperature, chopping rate, etc.) are fixed by experiment.

Figure 7 shows the results of the KMC simulations: we plot here the island density that would be observed if the largest mobile island were of size N_{max} . The computational load increases very rapidly with N_{max} and we therefore only considered islands of sizes less than or equal to 35. The data points follow very closely a power-law relation and we can thus extrapolate to larger values of N_{max} , i.e., smaller island densities. We find in this way that islands up to a maximum size of about 100 mono-clusters must be mobile in order to account for the observed island density of 1.1×10^{-5} per site. In what follows, we discuss in more detail the connection of this observation with experiment.

We first note that, in the gold-on-graphite experiments,¹² large islands form which are “partially ramified”, in the sense that the branch width is much larger than the size of the deposited clusters, each branch being formed by the coalescence of up to 200 monoclusters. In contrast, for antimony cluster deposition on graphite at room temperature,^{12,15} the islands are fully ramified, i.e., have a branch width identical to the diameter of the monoclusters; this establishes unambiguously that cluster coalescence is not taking place in this case. It has been shown, further, that the mobility of the islands is negligible in antimony.¹⁹ Our results suggest, therefore, when taken together with the work of Deltour *et al.*,⁷ that compact islands, which form through diffusion and coalescence, are mobile according to a $N^{-2/3}$ law. In contrast, ramified islands, which form when coalescence does not take place, have much reduced mobility — certainly much less than would be expected from a $N^{-2/3}$ law. N_{max} , therefore, signals

the crossover point between the two mobility regimes or, equivalently, the multicluster size at which the morphology of the islands crosses over from compact to ramified (or vice-versa). The physical reasons underlying the relation between mobility and morphology are not clear, but there appears to be no other ways to interpret the experimental results. This problem clearly deserves further studies.

To summarize this section, the mobility of large islands is evidently a *necessary* ingredient to account for the experimentally observed island density. Our simulations suggest that these islands can be as large as 100 monoclusters; while this is consistent with experiment, the exact value, as well as the precise dependence of the diffusion rate on size, cannot at present be estimated.

IV. CONCLUDING REMARKS

Cluster-deposition techniques are of great potential interest for assembling materials with specific, tailor-made applications. Yet, the fabrication process depends critically on the possibility for the clusters to diffuse on the surface in order to settle in appropriate positions, thus forming self-organized structures, or to aggregate/coalesce with other clusters in order to form larger-scale structures and eventually continuous layers. In this article, we have demonstrated, using molecular-dynamics simulations with realistic interatomic potentials, that the diffusion of large metallic clusters on graphite can take place at a pace which is quite comparable to that for single adatoms. We have also established that the rate of diffusion of cluster dimers can be very sizeable, comparable in fact to that for monoclusters. An extremely important consequence of this is that islands formed by the aggregation of clusters are also expected to be mobile. Using kinetic Monte Carlo simulations and assuming a proper scaling law for the dependence on size of the diffusivity of large clusters, we estimate that islands containing as much as 25 000 atoms (100 monoclusters) are expected to undergo diffusion at a significant rate on graphite surfaces. These findings have profound consequences for the morphology of cluster-assembled thin films.

ACKNOWLEDGMENTS

We are grateful to Laurent Bardotti, Art Voter and Tapio Ala-Nissila for useful discussions. This work was supported by the Natural Sciences and Engineering Research Council of Canada and the "Fonds pour la formation de chercheurs et l'aide à la recherche" of the Province of Québec. L.J.L. is grateful to the *Département de physique des matériaux de l'Université Claude-Bernard-Lyon-I*, where part of this work was carried out, for hospitality, support, and pleasant weather.

-
- ^(a) Electronic mail address: Laurent.Lewis@UMontreal.CA
 - ^(b) Electronic mail address: jensen@dpm.univ-lyon1.fr
 - ^(c) Electronic mail address: ncombe@dpm.univ-lyon1.fr
 - ^(d) Electronic mail address: barrat@dpm.univ-lyon1.fr
 - ¹ W. de Heer, *Rev. Mod. Phys.* **65**, 611 (1993).
 - ² Special issue on clusters, *Science* **271**, 920 (1996).
 - ³ O.H. Nielsen, J.P. Sethna, P. Stoltze, K.W. Jacobsen, and J.K. Nørskov, *Europhys. Lett.* **26**, 51 (1994).
 - ⁴ U. Röthlisberger, W. Andreoni, and M. Parrinello, *Phys. Rev. Lett.* **72**, 665 (1994).
 - ⁵ W.D. Luedtke and U. Landman, *J. Phys. Chem.* **100**, 13 323 (1996).
 - ⁶ L.J. Lewis, P. Jensen, and J.-L. Barrat, *Phys. Rev B* **56**, 2248 (1997).
 - ⁷ P. Deltour, J.-L. Barrat, and P. Jensen, *Phys. Rev. Lett.* **78**, 4597 (1997).
 - ⁸ J.C. Charlier, A. DeVita, X. Blase, and R. Car, *Science* **275**, 646 (1997).
 - ⁹ W.D. Luedtke and U. Landman, *Phys. Rev. Lett.* **82**, 3835 (1999).
 - ¹⁰ V. Paillard, P. Melinon, J.P. Perez, V. Dupuis, A. Perez, and B. Champagnon, *Phys. Rev. Lett.* **71**, 4170 (1993).
 - ¹¹ See for instance A. Perez, P. Melinon, V. Dupuis, P. Jensen, B. Prevel, J. Tuaille, L. Bardotti, C. Martet, M. Treilleux, M. Broyer, M. Pellarin, J.L. Vialle, and B. Palpant, *J. Physics D* **30**, 709 (1997).
 - ¹² P. Jensen, *Rev. Mod. Phys.* **71** (5), xxxxx (1999).
 - ¹³ A.S. Edelstein and R.C. Cammarata (Eds.), *Nanomaterials: Synthesis, Properties and Applications*, (IOP Publishing, Bristol, 1996); J.H. Fendler (Ed.), *Nanoparticles and Nanostructured Films* (Wiley-VCH, Weinheim, Germany, 1998).
 - ¹⁴ G. Fuchs, P. Melinon, F. Dos Santos Aires, M. Treilleux, B. Cabaud, and A. Hoareau, *Phys. Rev. B* **44**, 3926 (1991); C. Bréchnignac, Ph. Cahuzac, F. Carlier, C. Colliex, C. Mory, M. de Frutos, A. Masson, and B. Yoon, *Phys. Rev. B* **57**, R2084 (1998).
 - ¹⁵ L. Bardotti, P. Jensen, M. Treilleux, A. Hoareau, and B. Cabaud, *Phys. Rev. Lett.* **74**, 4694 (1995).
 - ¹⁶ A. Masson, J. J. Métois, and R. Kern, *Surf. Sci.* **27**, 463 (1971).
 - ¹⁷ M. Flüeli, P.A. Buffat, and J.-P. Borel, *Surf. Sci.* **202**, 343 (1988).
 - ¹⁸ Ph. Buffat and J.-P. Borel, *Phys. Rev. A* **13**, 2287 (1976); J.-P. Borel, *Surf. Sci.* **106**, 1 (1981).
 - ¹⁹ L. Bardotti, P. Jensen, M. Treilleux, A. Hoareau, and B. Cabaud, *Surf. Sci.* **367**, 276 (1996).
 - ²⁰ S.M. Foiles, M.I. Baskes, and M.S. Daw, *Phys. Rev. B* **33**, 7983 (1986).
 - ²¹ J. Tersoff, *Phys. Rev. B* **39**, 5566 (1989).
 - ²² A.F. Voter, *Phys. Rev. Lett.* **78**, 3908 (1997); *J. Chem. Phys.* **106**, 4665 (1997).
 - ²³ S. Pal and K. Fichthorn, *Chem. Eng. J.* **74**, 77 (1999).
 - ²⁴ M.S. Daw, S.M. Foiles, and M.I. Baskes, *Materials Science Reports* **9**, 251 (1993); S.M. Foiles in *Equilibrium Structure*

and Properties of Surfaces and Interfaces, ed. by A. Gonis and G.M. Stocks (Plenum, New York, 1992) p.89.

- ²⁵ H. Raffi-Tabar, H. Kamiyama, and M. Cross, Surf. Sci. **385**, 187 (1997); G.W. Wu and K.Y. Chan, Surf. Sci. **365**, 38 (1996); S.Y. Liem and K.Y. Chan, Surf. Sci. **328**, 119 (1995).
- ²⁶ See for instance D. Frenkel and B. Smit, *Understanding Molecular Simulation* (Academic Press, San Diego, 1996); M.P. Allen and D.J. Tildesley, *Computer Simulation of Liquids* (Clarendon Press, Oxford, 1987).
- ²⁷ Three different estimates of $r^2(t)$ are presented in Fig. 2: using the full extent of the run, only the first half, and only the second half. They are almost undistinguishable on this log-log plot.
- ²⁸ T. Hjelt, I. Vattulainen, T. Ala-Nissila and S.C. Ying, Surf. Sci., to be published.
- ²⁹ P. Jensen, N. Combe, J.L. Barrat, H. Larralde, C. Misbah, and A. Pimpinelli, Eur. Phys. J. B **11**, 497 (1999).
- ³⁰ P. Jensen and B. Niemeyer, Surf. Sci. Lett. **384**, 823 (1997).
- ³¹ N. Combe and P. Jensen, Phys. Rev. B **57**, 15 553 (1998).

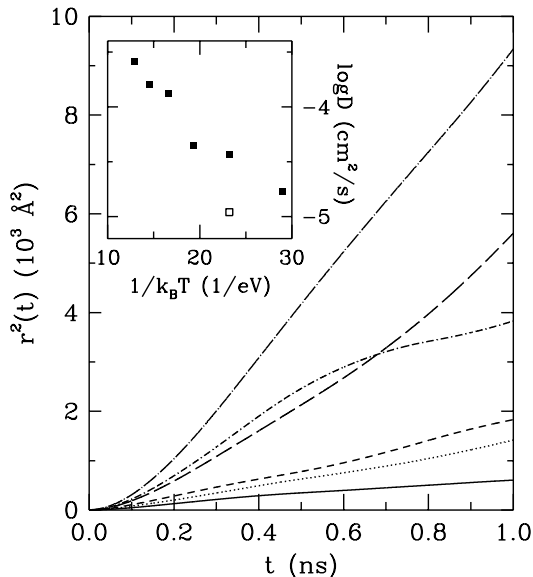


FIG. 1. Main figure: Time-averaged mean-square displacements for the cluster's center-of-mass at the various temperatures investigated, namely, from bottom to top, 400, 500, 600, 700, 800 and 900 K. (The 700 and 800 K curves are inverted for $t > 0.7$ ns). Inset: Arrhenius plot of the diffusion coefficient. The open square at 500 K ($1/k_B T = 23.2$ eV $^{-1}$) is the result for the frozen substrate.

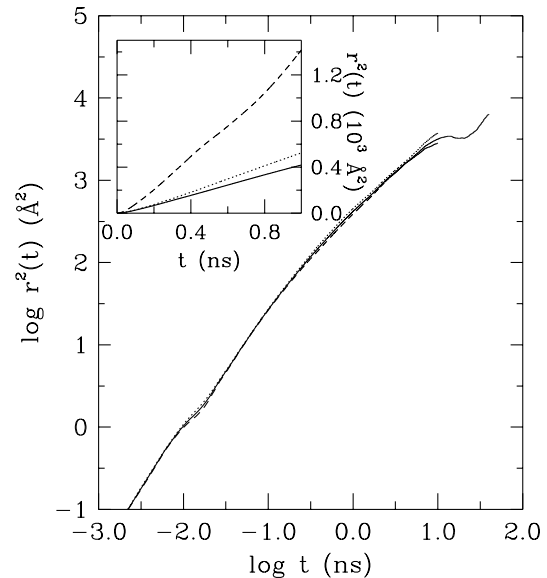


FIG. 2. Main figure: Log-log plot of the time-averaged mean-square displacements for the cluster's center-of-mass on the static substrate at 500 K. The three curves correspond to different estimates: using the full extent of the run (full curve); only the first half (dashes); only the second half (dots). The difference between these curves gives a measure of the error on the estimated diffusion coefficient. Inset: Time-averaged mean-square displacements for the monocluster on a static substrate (full line), the monocluster on a dynamic substrate (dashes) and the dicluster on a static substrate (dots).

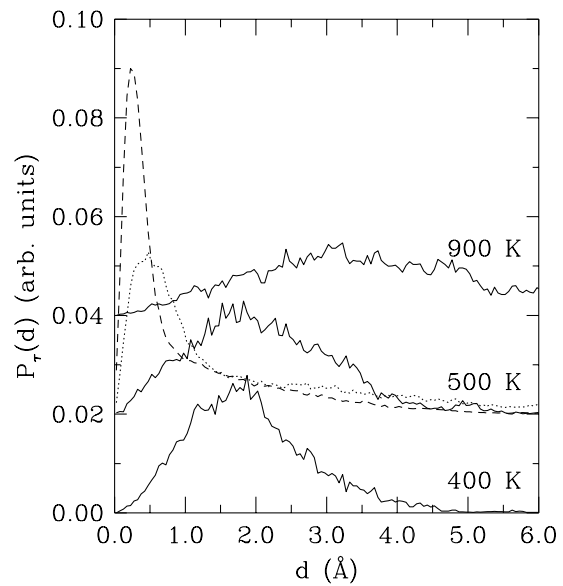
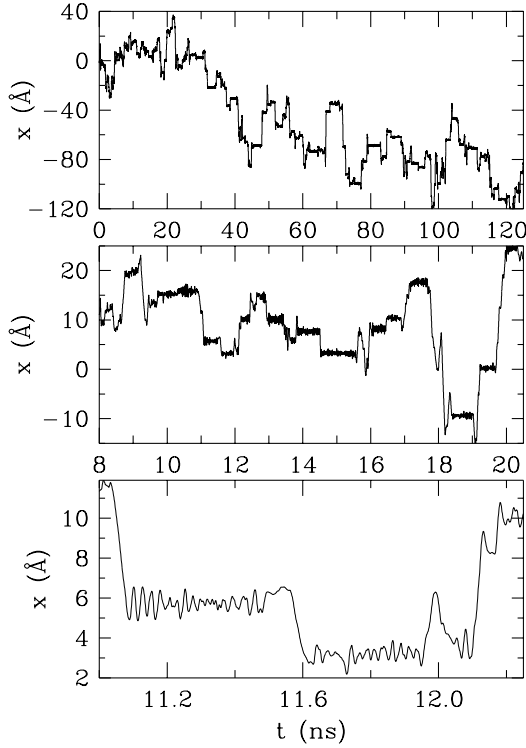
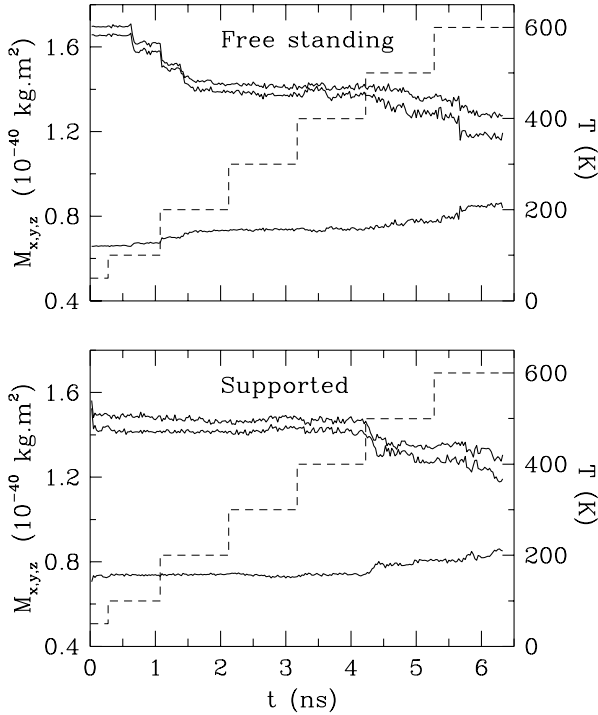


FIG. 3. The function $P_\tau(d)$, which gives the distribution of displacements of length d over a timescale of τ , at three different temperatures, as indicated. At 500 K, the three curves correspond to the monocluster on a dynamic substrate (full line), the monocluster on a static substrate (dashes) and the dicluster on a static substrate (dots).



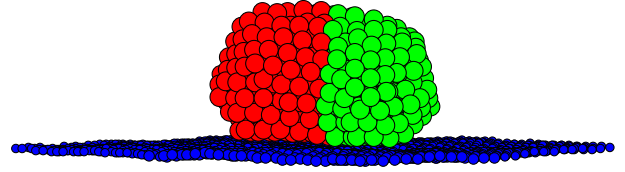
Lewis et al, Figure 4

FIG. 4. The x position of the cluster's center of mass at 500 K on a frozen substrate for three different timescales, showing the apparently self-similar character of the trajectory.



Lewis et al, Figure 5

FIG. 5. Evolution with time-temperature of the three moments of inertia (full lines) of the dicluster, both free-standing and supported on graphite; the correspondence between temperature and time is indicated by the dashed, stepwise curve.



Lewis et al, Figure 6

FIG. 6. Ball-and stick model of the gold dicluster on the graphite substrate at 200 K, after the neck between the two monoclusters has formed completely. The two monoclusters are colored differently for ease of visualisation.

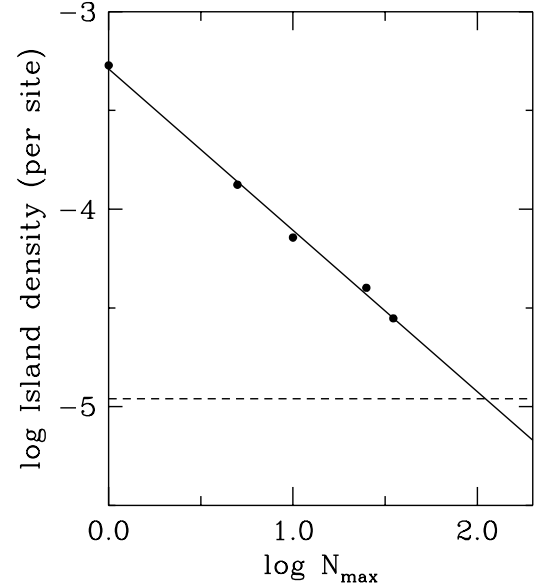


FIG. 7. Predicted island density as a function of the size N_{\max} of the largest multi-cluster island which is allowed to diffuse. The calculations were carried out using kinetic Monte Carlo simulations as discussed in the text. The full line is a linear fit to the data points and the dashed line indicates the experimental density.